Deactivation of Cu-SSZ-13 in the presence of SO$_2$ during hydrothermal aging

Yulong Shan[a,b], Xiaoyan Shi[a,b], Zidi Yan[a,b], Jingjing Liu[a,b], Yunbo Yu[a,b,c], Hong He[a,b,c,*]

[a] State Key Joint Laboratory of Environment Simulation and Pollution Control, Research Center for Eco-Environmental Sciences, Chinese Academy of Sciences, Beijing, 100085, China
[b] University of Chinese Academy of Sciences, Beijing, 100049, China
[c] Center for Excellence in Regional Atmospheric Environment, Institute of Urban Environment, Chinese Academy of Sciences, Xiamen, 361021, China

ABSTRACT

Cu^{2+}-exchanged zeolite catalysts with the chabazite (CHA) structure have been thought to be optimal candidates for selective catalytic reduction of NOx with NH$_3$. In real applications, however, SCR catalysts readily undergo hydrothermal aging and sulfur poisoning. In this work, the co-effect of SO$_2$ and hydrothermal aging at high temperature was investigated. Different from the reversible inhibition of SO$_2$ poisoning that occurs at low temperatures, the sulfur poisoning at high temperature is permanent due to the destruction of the zeolite structure, and no deposit of sulfate is observed. Cu-SSZ-13 catalysts were characterized through solid state ^{27}Al nuclear magnetic resonance (^{27}Al-NMR), X-ray diffraction (XRD), temperature-programmed desorption of NH$_3$ and NO (NH$_3$/NO-TPD), electron paramagnetic resonance (EPR), temperature-programmed reduction by H$_2$(H$_2$-TPR), in situ DRIFTS, and thermogravimetric analysis with mass spectrometric detection (TG-Mass) to develop an understanding of the degradation mechanisms during hydrothermal aging and sulfurization at high temperature. The results indicated that SO$_2$ dislodged the extra-framework Al atoms that resulted from the dealumination process that occurs during hydrothermal aging. More Cu^{2+} species were accumulated as CuOx for Cu-SSZ-13 after sulfurization at high temperature compared to that treated by hydrothermal aging only. The dealumination and accumulation of Cu^{2+} species caused a loss of acid and active sites for the Cu-SSZ-13 catalyst, and resulted in degradation of NH$_3$-SCR performance.

1. Introduction

Various technologies have been developed for the abatement of NOx from diesel engines. Among these, selective catalytic reduction of NOx with NH$_3$ (NH$_3$-SCR) is a widely used technique [1]. As the core of the NH$_3$-SCR technique, the Cu^{2+} ion-exchanged SSZ-13 (Cu-SSZ-13) catalyst, a zeolite with the chabazite (CHA) structure, has attracted much interest over the past several years due to its good NH$_3$-SCR performance and exceptional hydrothermal stability [2–5]. Numerous studies have been carried out to learn the distribution and state of Cu^{2+} species, reaction mechanism and reasons for the excellent hydrothermal stability via a variety of characterization methods, such as H$_2$-TPR, NMR, EPR, XANES and FT-IR techniques [4,6–10].

However, in actual application, SCR catalysts readily undergo hydrothermal aging and sulfur poisoning [3,4,11–13]. The hydrothermal aging typically takes place when the SCR catalysts are exposed to the high temperature exhaust containing humidity during the regeneration of the diesel particulate filter (DPF). The Cu-SSZ-13 zeolite catalysts always suffered irreversible damage such as dealumination of the

framework structure and accumulation of Cu^{2+} species when subjected to sufficiently high temperatures [3,4,8]. These changes are closely related to the degradation of NH$_3$-SCR performance. The sulfur poisoning occurs when the catalyst is exposed to SO$_2$ and SO$_3$, which is generated from oxidation of sulfur-containing compounds in the diesel fuel. Cu-SSZ-13 zeolite catalysts are significantly sensitive to sulfur poisoning. Many studies reported that SO$_2$ severely inhibited low-temperature NH$_3$-SCR performance over Cu-SSZ-13 due to the formation of ammonium-sulfur species, which blocked the active sites [12–16]. Unlike the permanent damage caused by hydrothermal aging, sulfur poisoning could be reversed via the decomposition of deposited sulfate species by elevated temperature treatment [14,15,17]. Overall, hydrothermal aging and sulfur poisoning are two vital factors that deteriorate the Cu-SSZ-13 catalyst NH$_3$-SCR performance. However, the influences of hydrothermal aging and sulfur poisoning are always discussed separately. The co-effect of hydrothermal aging and SO$_2$ at high temperatures has been little studied. In fact, the regeneration of the DPF takes place accompanied with SO$_2$ formation from substances accumulated on the DPF, which goes through the SCR catalysts together

with the exhaust [18]. Hence, the presence of SO_2 should be taken into account during the hydrothermal aging process for SCR catalysts.

In the present study, our purpose is to investigate the deactivation of one-pot method synthesized Cu-SSZ-13 using SO_2 exposure under severe hydrothermal aging conditions. Through the use of characterization techniques such as XRD, ^{27}Al-NMR, TPD, EPR, H_2-TPR, DRIFTS using NH_3 as a probe molecule and TG-Mass, we observed how the framework structure of the zeolite and the acid and active sites changed when SO_2 was introduced during hydrothermal aging, thereby providing guidance for further SCR catalyst design and advanced control technologies to minimize and avoid deterioration.

2. Experimental

2.1. Catalyst synthesis

The initial Cu-SSZ-13 catalyst sample was synthesized using the one-pot synthesis method reported previously by Xiao's and our group [5]. The composition of the gel was as follows: 4 Cu-TEPA:14.8 Na_2O:3.0 Al_2O_3:30 SiO_2:600 H_2O. The initial Cu-SSZ-13 with excess Cu loading was obtained after crystallization at 140 °C for 4 days. Next, the sample was ion-exchanged with HNO_3 solution (pH = 2) twice, then filtered, washed with distilled water and dried at 100 °C overnight. After calcination in an oven at 600 °C for 6 h with a ramp rate of 10 °C/min, The obtained catalysts were denoted as the fresh Cu-SSZ-13 (FR-Cu-SSZ-13). Then, the fresh Cu-SSZ-13 was hydrothermally aged in 10% H_2O/air and sulfated in (10% H_2O + 100 ppm SO_2)/air at 750 °C for 32 h, and denoted as HA-Cu-SSZ-13 and SA-Cu-SSZ-13, respectively.

2.2. NH₃-SCR activity test

Catalyst activities were determined in a fixed-bed quartz flow reactor at atmospheric pressure. The reaction conditions were controlled as follows: 500 ppm NO, 500 ppm NH_3, 5 vol.% O_2, balance N_2, 5 vol.% H_2O and the total flow rate was held at 500 mL/min. Catalyst samples (about 50 mg) of 40–60 mesh size were used, with gas hourly space velocity (GHSV) estimated as 400,000 h^{-1}. The exhaust gas was continuously analyzed by an online Nicolet Is10 spectrometer equipped with a heated, low volume (0.2 L) multiple-path gas cell (2 m). FTIR spectra were collected throughout and the results were recorded when the SCR reaction reached a steady state. The NOx and NH_3 conversions were calculated as follows:

$$NO_x \text{conversion} = \left(1 - \frac{[NO_x]_{out}}{[NO_x]_{in}}\right) \times 100\%$$

$$NH_3 \text{conversion} = \left(1 - \frac{[NH_3]_{out}}{[NH_3]_{in}}\right) \times 100\%$$

2.3. Catalyst characterization

Powder X-ray diffraction (XRD) measurements were carried out on a computerized PANalytical X'Pert Pro diffractometer with Cu Kα (λ = 0.15406 nm) radiation. The data of 2θ from 5° to 40° were collected with the step size of 0.02°.

N_2 adsorption/desorption isotherms of the series of Cu-SSZ-13 catalysts were measured using a Micromeritics ASAP 2020 system to obtain the specific surface areas and pore volume. Prior to the N_2 physical adsorption, the samples were degassed at 300 °C for 5 h. Micropore area and micropore volume were determined by the t-plot method.

The solid state ^{27}Al MAS NMR spectra were recorded on a Bruker AVANCE III 400 WB spectrometer equipped with a 4 mm standard bore CP MAS probe head whose X channel was tuned to 104.27 MHz for ^{27}Al, using a magnetic field of 9.39T at 297 K. The dried and finely powdered samples were packed in the ZrO_2 rotor closed with a Kel-F

cap, which was spun at 12 kHz rate. A total of 1000 scans were recorded with 2 s recycle delay for each sample. All ^{27}Al MAS chemical shifts are referenced to the resonances of an aluminum oxide (Al_2O_3) standard (d = 11.5).

Temperature-programmed desorption with NH_3 and NO (NH_3-TPD and NO-TPD) experiments were performed as part of the NH_3-SCR activity measurement. 30 mg of catalyst was pre-treated in air with 20% O_2/N_2 for 1 h at 500 °C and then cooled down to 35 °C. Afterwards, the sample was placed into an atmosphere of 500 ppm NH_3(NO)/N_2, followed by N_2 purging for 1 h. Finally, the temperature was raised to 600 °C in N_2 at the rate of 10 °C/min and the production of NH_3(NO) was detected.

The electron paramagnetic resonance (EPR) spectra of the samples were recorded at 155 K on a Bruker E500 X-band spectrometer. The fresh samples were pretreated at 400 °C for 2 h in 20 vol% O_2/N_2 to obtain dehydrated samples. For measurement, all samples were placed into quartz tubes.

Temperature-programmed reduction with hydrogen (H_2-TPR) experiments were carried out on a Micromeritics AutoChem 2920 chemisorption analyzer. A liquid nitrogen cold trap placed before the detector was used to eliminate the interference of H_2O. 50 mg of the samples were pre-treated in a quartz reactor in air with the flow rate of 50 mL/min at 500 °C for 1 h. After the catalyst was cooled down to room temperature, H_2-TPR was performed in a 10 vol% H_2/Ar gas flow of 50 mL/min at a heating rate of 10 °C/min.

The in situ DRIFTS experiments were performed using an FTIR spectrometer (Nicolet Is10) equipped with a Smart Collector and MCT/A detector. The reaction temperature was controlled precisely by an Omega programmable temperature controller. Prior to each experiment, the catalyst was pretreated at 500 °C for 30 min in a flow of 20 vol.% O_2/N_2 and then cooled down to 35 °C. The background spectrum was collected in flowing N_2 and automatically subtracted from the sample spectrum. In order to identify the adsorbed species, the catalysts were exposed to a flow of 500 ppm NH_3/N_2 and then flushed with N_2. All spectra were recorded by accumulating 100 scans with a resolution of 4 cm^{-1}.

Thermogravimetric analysis was conducted on a METTLER TOLEDO STAR^e System equipped with a quadrupole mass spectrometer (MKS Cirrus) to explore the process of deposit decomposition on the catalysts. The signals of SO_2 (m/z = 64) and SO_3 (m/z = 80) were recorded. Samples were heated up to 1000 °C at a rate of 10 °C/min under a flow of 20% O_2/N_2.

3. Results and discussion

3.1. NH₃-SCR performance

The standard SCR NOx and NH_3 conversion activities of FR-Cu-SSZ-13, HA-Cu-SSZ-13 and SA-Cu-SSZ-13 catalysts are depicted in Fig. 1 as a function of temperature from 150 to 550 °C. It was apparent that the fresh Cu-SSZ-13 exhibited the best NH_3-SCR activity at all temperatures. The NO reduction activity declined to some extent for the Cu-SSZ-13 after it was hydrothermally aged at 750 °C for 32 h. Significant loss of NO reduction activity was observed for the SA-Cu-SSZ-13 sample that was hydrothermally aged in the presence of 100 ppm SO_2. This suggested that the deactivation of Cu-SSZ-13 during hydrothermal aging was much more severe in the presence of SO_2. At temperatures above 450 °C and 300 °C for the HA-Cu-SSZ-13 and SA-Cu-SSZ-13 samples, the NH_3 conversion is much higher than NO conversion due to unselecticve NH_3 oxidation. The unselective NH_3 oxidation was primarily responsible for the decay of NO conversion at high temperatures.

It has been generally recognized that the hydrothermal aging damages the zeolite structure framework and results in the formation of CuOx [3,4], while SO_2 was usually thought to form sulfate-like species on the catalyst surface, especially at low temperatures [12,16]. Therefore, considering the high temperature when introducing SO_2 under
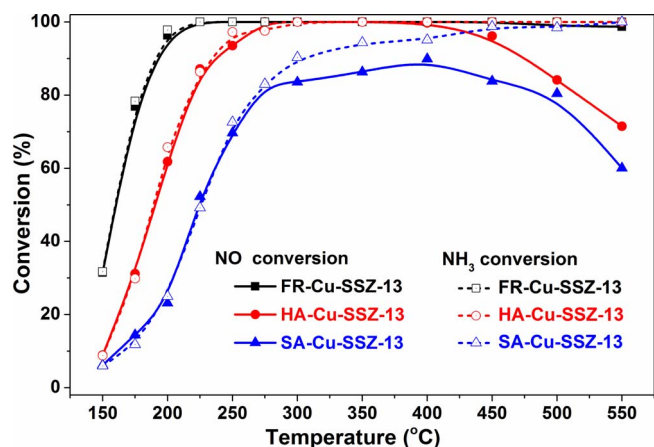
Fig. 1. NOx and NH$_3$ conversion of FR-Cu-SSZ-13, HA-Cu-SSZ-13, and SA-Cu-SSZ-13 catalysts under standard SCR conditions. [NO] = [NH$_3$] = 500 ppm, 5 vol.%O$_2$, 5 vol.% H$_2$O, balance N$_2$. GHSV = 400,000 h^{-1}.

hydrothermal aging conditions, collapse of the zeolite structure and accumulation of Cu^{2+} species may take place.

3.2. Crystal structure of zeolite

The N$_2$ adsorption-desorption isotherms are shown in Fig. 2. All the samples showed curves typical of microporous materials. The t-Plot micropore areas and volumes are also tabulated in Table 1. After hydrothermal aging and sulfuration, the micropore area of Cu-SSZ-13 catalysts decreased from 439 m^2/g (fresh Cu-SSZ-13) to 242 m^2/g (HA-Cu-SSZ-13) and 190 m^2/g (SA-Cu-SSZ-13), respectively. The same trend was also observed for the micropore volume. These observations indicated that the presence of SO$_2$ intensified the damage to the pore structure and framework of the zeolites during hydrothermal aging.

To probe the zeolite structure of the tested samples, XRD profiles were measured and are shown in Fig. 3. The typical peaks of the CHA structure remained intact for the HA-Cu-SSZ-13 sample, with a slight decrease of crystallinity. This suggested that the framework of Cu-SSZ-13 was stable when subjected to hydrothermal aging at 750 °C for 32 h. However, all the diffraction peaks of the SA-Cu-SSZ-13 catalyst showed a significant decline, indicating that the framework of Cu-SSZ-13 was severely damaged by hydrothermal aging in the presence of SO$_2$. It was noted that the diffraction peaks of CuOx were scarcely observed over
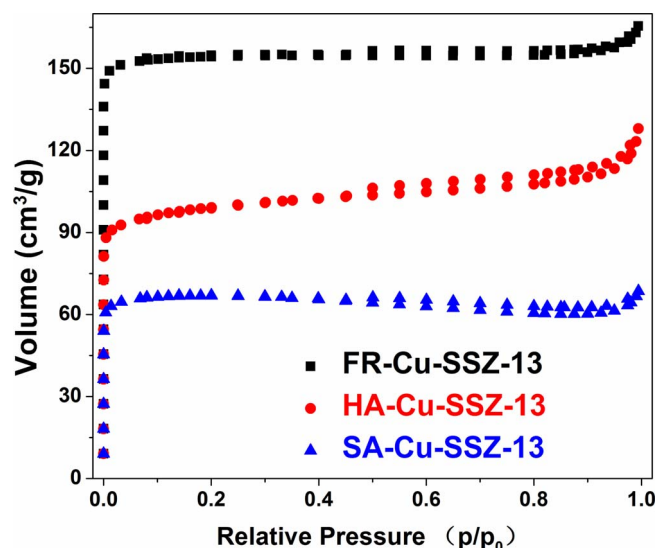

Fig. 2. N$_2$ adsorption-desorption isotherms of the FR-Cu-SSZ-13, HA-Cu-SSZ-13, and SA-Cu-SSZ-13 catalysts.

Table 1
Micropore areas and volumes of the catalysts.

Samples	Micropore areas (m^2/g)	Micropore volumes (m^3/g)
FR-Cu-SSZ-13	439	0.231
HA-Cu-SSZ-13	242	0.127
SA-Cu-SSZ-13	190	0.100

the HA-Cu-SSZ-13 and SA-Cu-SSZ-13 samples. However, one should be cautious in interpreting these results as signifying no formation of CuOx, since the size of the CuOx formed might be too small to be detected in XRD profiles [2,19].

The XRD indicated the degradation of the long-range ordered structure after aging. Furthermore, solid state ^{27}Al-NMR is more sensitive than XRD to changes in the local Al environment. As shown in Fig. 4, there were two peaks in the ^{27}Al-NMR profiles. The features at 58 ppm and 0 ppm were attributed to the framework tetrahedral Al and extra-framework octahedral Al, respectively [3,20,21]. For the FR-Cu-SSZ-13 catalyst, almost all Al was tetrahedral, while only a small amount of extra-framework Al was observed. After experiencing hydrothermal aging, regardless of the presence of SO$_2$, a dramatic decline of tetrahedral Al was observed, due to the dealumination process. The removal of Al caused the breakup of the zeolite framework structure and resulted in the loss of NO conversion activity. The reason that octahedral Al formed by the migration of tetrahedral Al was not observed was ascribed to the strong interaction with paramagnetic Cu ions [3]. The ^{27}Al-NMR results suggest that the presence of SO$_2$ promoted the dealumination process to some degree during the hydrothermal aging.

However, it is worth noting that only a subtle difference in dealumination was observed for the HA-Cu-SSZ-13 and SA-Cu-SSZ-13 samples compared to the significant difference in peak intensity in the XRD profiles between the two samples. It is generally known that the X-ray diffraction gives information on the long-range order of zeolites, while the NMR technique is sensitive to probing the local Al environment. In previous studies, Fickel et al. and Blakeman et al. found that the dealumination process of small-pore zeolites during hydrothermal aging was inhibited because the constricting dimensions of the small pores limited the detachment of aluminum hydroxide [6,22]. From the results of BET, more destruction of the pore structure for SA-Cu-SSZ-13 catalysts was observed compared to the HA-Cu-SSZ-13 catalysts. Therefore, the dealumination process removed only a small part of Al atoms for the HA-Cu-SSZ-13 samples during the hydrothermal aging due to the constriction of the integrated pore structure, and HA-Cu-SSZ-13 maintained its long-range order structure for the retention of Al atoms. However, for the SA-Cu-SSZ-13 samples with more severely damaged pore structure, the removal of a large number Al atoms due to the loss of this constricting function degraded its long-range order patterns. Therefore, the presence of SO$_2$ dislodged the Al atoms that resulted from dealumination during the hydrothermal aging process, and further destroyed the zeolite long-range order structure. Giving a more profound impact, SO$_2$ caused the collapse of the zeolite structure and irreversible destruction of the catalysts.

3.3. Acid sites and active sites

3.3.1. NH$_3$-TPD and NO-TPD analysis

The NH$_3$-TPD technique was used to explore the acid sites of the Cu-SSZ-13 with different aging conditions as shown in Fig. 5(A). The calculated amount of NH$_3$ is also listed in Table 2. Obviously, the NH$_3$ storage decreased as the hydrothermal aging conditions became more severe. Quantitatively, the amount of NH$_3$ storage was 2400 μmol/g for HA-Cu-SSZ-13 and 1290 μmol/g for the SA-Cu-SSZ-13 catalyst, which was significantly decreased compared to fresh sample with the NH$_3$ storage of 5163 μmol/g. It indicated that in the presence of SO$_2$, hydrothermal aging made Cu-SSZ-13 lose much more acid sites compared
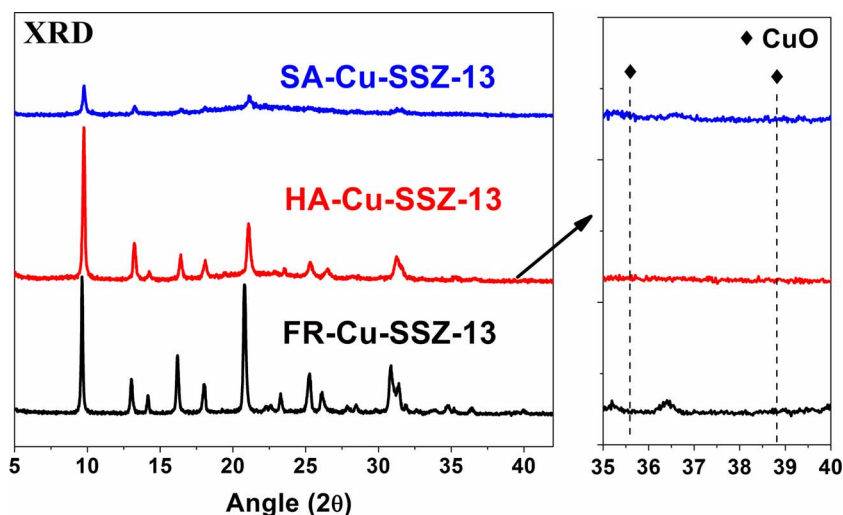
Fig. 3. XRD patterns of the FR-Cu-SSZ-13, HA-Cu-SSZ-13, SA-Cu-SSZ-13 catalysts.
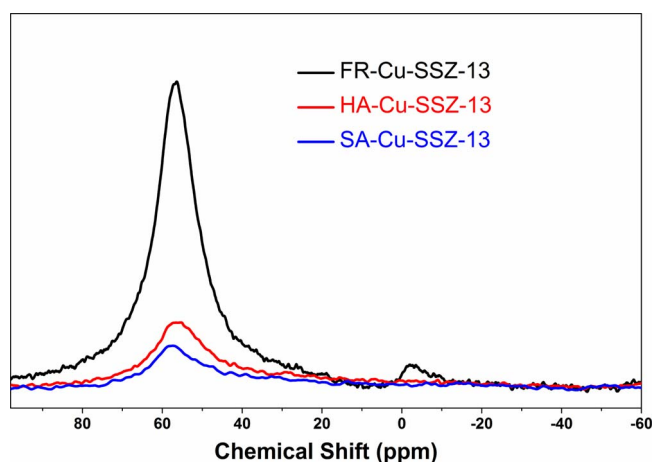

Fig. 4. ^{27}Al-NMR spectra of FR-Cu-SSZ-13, HA-Cu-SSZ-13, and SA-Cu-SSZ-13 catalysts.

Table 2
The amounts of NH_3 and NO desorbed in the TPD experiments.

samples	NH_3 (μmol/g)	NO (μmol/g)
FR-Cu-SSZ-13	5163	269
HA-Cu-SSZ-13	2400	56
SA-Cu-SSZ-13	1290	20

and the peaks at 275 °C and 425 °C were assigned to strong Lewis acid sites (Cu ion sites) and Brønsted acid sites (Si-OH-Al), respectively [23–25]. The remarkable decrease in Cu ions sites for SA-Cu-SSZ-13 suggested significant change in the Cu^{2+} state. This phenomenon was also observed in the NO-TPD results shown in Fig. 5(B), and the NO absorption amounts tabulated in Table 2. Compared to NO storage of fresh sample (269 μmol/g) and HA-Cu-SSZ-13 sample (56 μmol/g), there was only 20 μmol/g NO storage on the SA-Cu-SSZ-13 sample, indicating that Cu^{2+} active sites were poisoned much more heavily after hydrothermal aging with SO_2 at hight temperartures, since NO is always adsorbed onto the Cu^{2+} active sites[9,26]. Meanwhile, the total number of Brønsted acid sites decreased sharply after aging for HA-Cu-SSZ-13 and SA-Cu-SSZ-13 owing to the dealumination process, which was proved by the ^{27}Al-NMR results. The NH_3-TPD and NO-TPD results

to that under hydrothermal aging conditions without SO_2. In detail, three peaks were found in the NH_3-TPD profiles. Acoording to previous studies, the desorption at 150 °C was ascribed to weakly adsorbed NH_3,
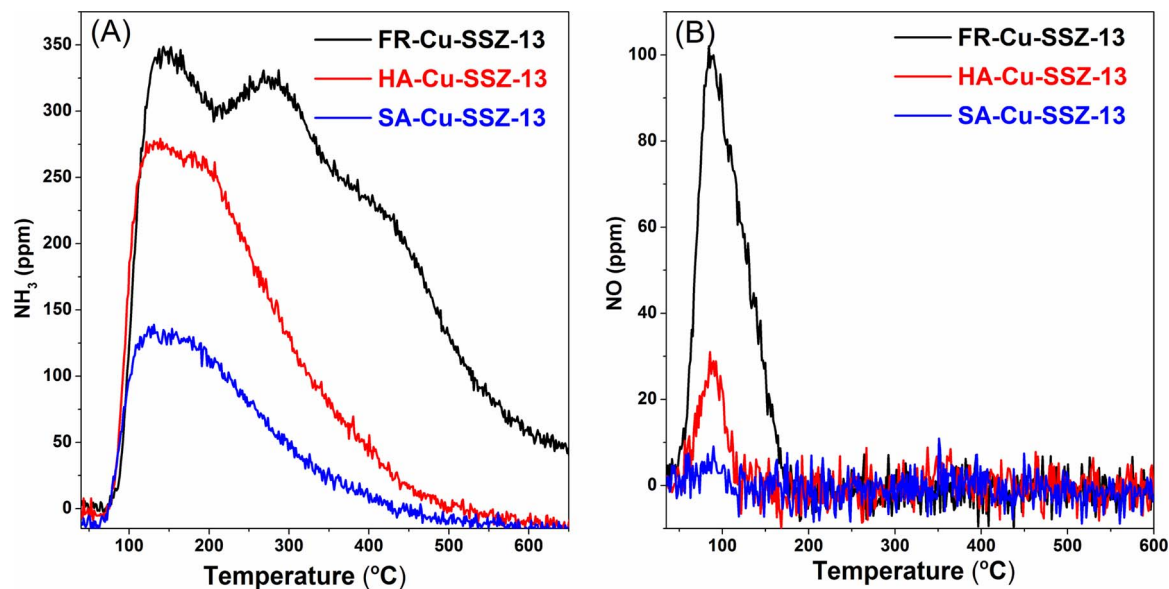

Fig. 5. NH_3-TPD (A) and NO-TPD (B) profiles of FR-Cu-SSZ-13, HA-Cu-SSZ-13, and SA-Cu-SSZ-13 catalysts.

gave strong evidence that the addition of SO_2 during the hydrothermal aging decrease more NH_3 and NO storage compared to that under hydrothermal aging conditions without SO_2. The presence of SO_2 not only intensified the dealumination, but more importantly, changed the state of Cu^{2+} species, and led to the deactivation of Cu-SSZ-13.

3.3.2. The change of Cu^{2+} species measured by EPR and H_2-TPR analysis

To investigate the state of Cu^{2+} ions in the zeolite, an EPR experiment was carried out at 155 K. Gao et al. [27,28] reported on the changes in the EPR signal of Cu-SSZ-13 catalysts with different Cu loadings and at different temperatures. They argued that the peaks in the high field and the definition of low-field hyperfine structures could explain the Cu^{2+} ion mobility. Kim et al. [4] classified the Cu^{2+} ions into three distinct species in the low-field hyperfine structures: α, β, and γ species. As depicted in Fig,6A in the high field, two resolved peaks at 3280 and 3320 G were observed for HA-Cu-SSZ-13 and SA-Cu-SSZ-13, while the FR-Cu-SSZ-13 showed only one peak. This is ascribed to the high mobility of Cu^{2+} ions in the HA-Cu-SSZ-13 and SA-Cu-SSZ-13 catalysts since the severe aging conditions decreased the interaction between the Cu^{2+} ions and the CHA framework [28]. The more highly resolved peaks at high field for the SA-Cu-SSZ-13 indicated that SO_2 strongly deteriorated the interaction between the Cu^{2+} ions and the CHA framework during the hydrothermal aging. Additionally, by analyzing the hyperfine features in the low field region, three species were found, as illustrated in Fig. 6B, and the peak assignments are listed in Table 3 [4]. It was observed that the peak patterns shifted to high field with increasing severity of hydrothermal aging. The spectra of the FR-Cu-SSZ-13 catalyst showed two peaks (g = 2.402 and g = 2.372), assigned to Cu^{2+} in D6R cages and CHA cages, repectively. After undergoing hydrothermal aging, HA-Cu-SSZ-13 showed three peaks, containing Cu^{2+} in D6R cages, Cu^{2+} in CHA cages, and Cu^{2+}-Al_2O_3 species, indicating that Cu^{2+} accumulated to form CuOx with the concomitant dealumination process. However, SA-Cu-SSZ-13 primarily showed a prominent peak for Cu^{2+}-Al_2O_3 species, demonstrating that hydrothermal aging in the presence of SO_2 resulted in more severe deactivation of the Cu^{2+} active sites, which was closely related to the degradation of NH_3-SCR performance.

The changes in Cu^{2+} active sites could also be comfirmed by H_2-

Table 3
Cu^{2+} species based on the EPR analysis.

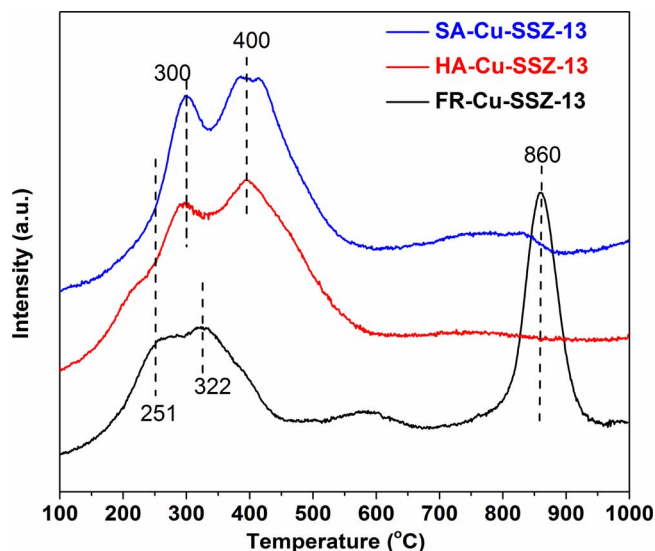| Species	Cu^{2+} state	g	A
α	Cu^{2+}-D6R	2.402	125
β	Cu^{2+}-CHA	2.372	146
γ	Cu^{2+}-Al_2O_3	2.321	166

Fig. 7. H_2-TPR profiles of FR-Cu-SSZ-13, HA-Cu-SSZ-13, and SA-Cu-SSZ catalysts.

TPR results shown in Fig. 7. The peaks of fresh Cu-SSZ-13 located at 251, 322, and 860 °C are attributed to the reduction of Cu^{2+} to Cu^+ in the CHA cages (β species), D6R cages (α species) and Cu^+ to Cu^0. [4,7] For the HA-Cu-SSZ-13 and SA-Cu-SSZ-13 catalysts, no reduction of Cu^+ to Cu^0 at high temperatures was observed. This absence of reduction indicted that the reduction of Cu^{2+} only needed one step, instead of two steps consisting of Cu^{2+} to Cu^+ and Cu^+ to Cu^0. Therefore, the
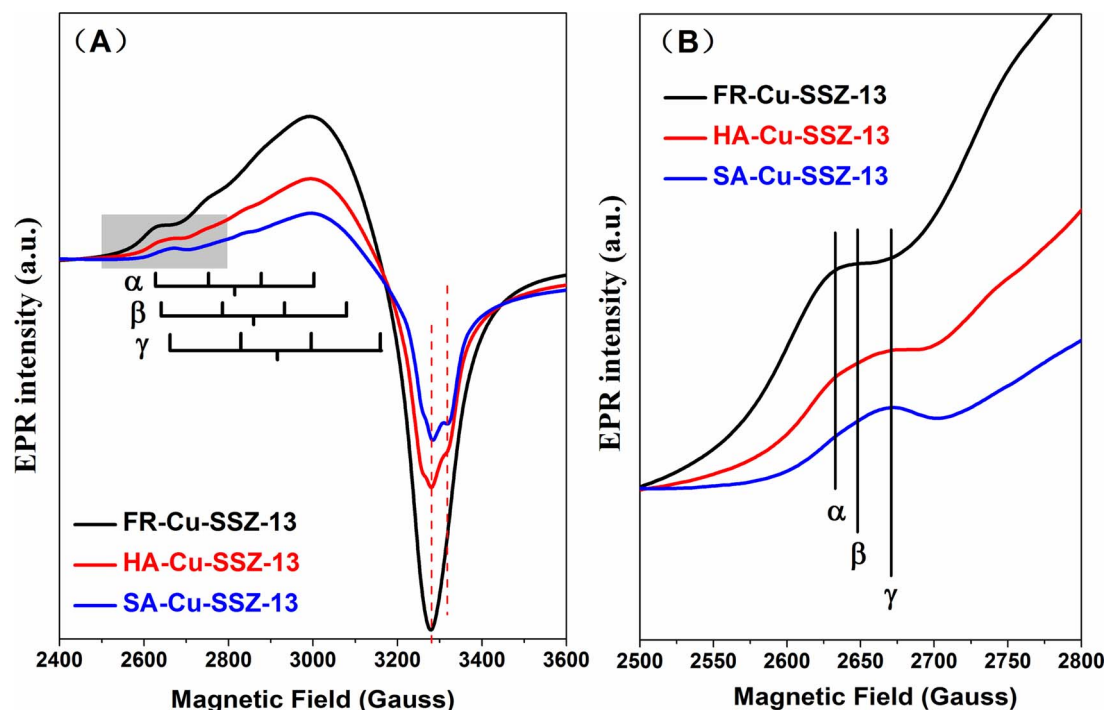

Fig. 6. EPR profiles of FR-Cu-SSZ-13, HA-Cu-SSZ-13, and SA-Cu-SSZ-13 catalysts.
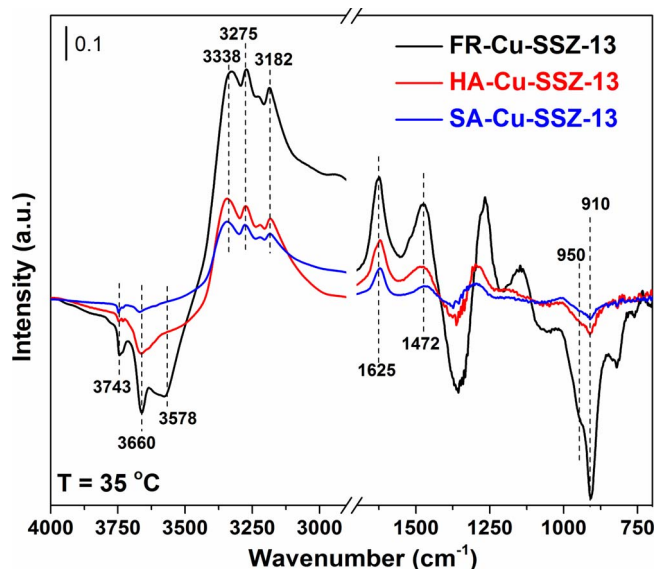
Fig. 8. DRIFTS spectra of adsorbed NH_3 on FR-Cu-SSZ-13, HA-Cu-SSZ-13, and SA-Cu-SSZ-13 catalysts. 35 °C exposure to 500 ppm NH_3 and a balance of N_2, total flow rate 300 mL/min.

peaks at 300 and 400 °C are primarily ascribed to CuO for the HA-Cu-SSZ-13 and SA-Cu-SSZ-13 catalysts [5,27]. In addition, much more CuO formation was observed for the SA-Cu-SSZ-13 catalyst, indicating that SO_2 promoted the accumulation of CuO.

In summary, combining the analysis of XRD and ^{27}Al-NMR results, we speculated that the presence of SO_2 promoted the mobility of Al atoms resulting from dealumination during hydrothermal aging, and these easily-removable Al atoms led more Cu^{2+} species to accumulate readily.

3.3.3. in situ DRIFTS spectra of NH_3 adsorption

To gain further insight into the nature of the acidic and active sites, the DRIFT spectra of the NH_3 adsorbed onto the Cu-SSZ-13 samples was shown in Fig. 8. The probe molecule NH_3 was used due to its specific adsorption on zeolite Brønsted acid sites and Cu active sites. As depicted in Fig. 8, the negative bands at 3743 and 3660 cm^{-1} were attributed to NH_3 adsorbed on the external Si-OH and Al-OH groups. [13,23] The decay of the peak at 3578 cm^{-1} was ascribed to the weakening of the stretching vibrations of the Al-OH-Si group, together with the appearance of new features of 1472, 3338 and 3275 cm^{-1}, which related to NH_4^+ on Brønsted acid sites [23,29,30]. The bands at 3182 and 1625 cm^{-1} were assigned to NH_3 adsorbed on Lewis acid sites (such as Cu^{2+}) [15,25,31]. Additionally, the vibrations below 1000 cm^{-1} could be classified into the zeolite T-O-T bond vibration region to probe the interaction between Cu ions and zeolite framework structure. In detail, the bands at 950 and 910 cm^{-1} represented the zeolite T-O-T vibration perturbed by Cu^{2+} in CHA and D6R cages, respectively. Morever, the lower the peak was, the stronger the interaction of Cu ions with the zeolite framework structure [7,13,25,32]. The adsorbed NH_3 species observed on the Cu-SSZ-13 catalysts before and after aging showed significant differences for the three samples.

Regarding the O−H bond stretching region at 3743, 3660 and 3578 cm^{-1}, it was obvious that the addition of SO_2 during the hydrothermal aging reduced the amount of acid sites, especially the Brønsted acid sites (3578 cm^{-1}), by comparing the spectra of HA-Cu-SSZ-13 and SA-Cu-SSZ-13. As the O−H bands decreased, a concomitant increase of the bands for N−H bending at 3100–3400 cm^{-1} and 1400–1700 cm^{-1} was also observed. The same trend of reduction of acid sites was seen for addition of SO_2 when undergoing hydrothermal aging. These results showed good agreement with the NH_3 adsorption in the NH_3-TPD experiment. It was noteworthy that the T-O-T vibration perturbed by

Cu^{2+} at 850–1000 cm^{-1} could reflect the influence of the Cu ion state. The intensity of the negative peak at 950 cm^{-1} dramatically weakened after hydrothermal aging. Further, the peak almost disappeared for HA-Cu-SSZ-13, which was also seen in the H_2-TPR result. On the other hand, whether the Cu was in the CHA cage or the D6R cage, the introduction of SO_2 impaired the interaction of Cu ions with the zeolite framework more seriously for the SA-Cu-SSZ-13 compared to the HA-Cu-SSZ-13 sample. Therefore, combined with the H_2-TPR results, we concluded that the hydrothermal aging process prompted the Cu-SSZ-13 catalyst to convert Cu ions to CuOx and weakened the interaction of Cu ions with the zeolite framework. Notably, exposure to SO_2 aggravated the deactivation of Cu active sites. The DRIFTS of NH_3 absorption clearly identified the deterioration of acid sites and active sites during the hydrothermal aging whether or not SO_2 was present.

3.4. Sulfur deposition test

There have been many studies on sulfur poisoning of Cu-SSZ-13 catalysts, and generally conclusions were drawn that SO_2 inhibits the NH_3-SCR reaction of catalysts, especially at low temperatures, due to sulfate accumulation on the catalysts [12,16,17]. Additionally, the recovery of sulfated Cu-SSZ-13 catalysts was observed with elevated temperature treatment for the decomposition of part of the sulfate [14–16]. Therefore, thermogravimetric analysis combined with mass spectrometric detection of evolved species was used to explore the deposition of sulfur on the SA-Cu-SSZ-13 catalyst, and the profiles are shown in Fig. 9. There was no weight loss up to 1000 °C except for the elimination of H_2O before 150 °C, indicating that no decomposition of deposits occurred. In addition, in the mass spectra, the SO_2 and SO_3 signals remained constant over the whole temperature range, meaning that there was no sulfate accmulation for the SA-Cu-SSZ-13 catalysts. Indeed, in this work, the sulfurization took place at the relatively high temperature of 750 °C in the presence of water, where many sulfate species, including Al-SO$_4$, Cu-SO$_4$, (NH$_4$)$_2$SO$_4$ and H_2-SO$_4$ are unstable and decompose below 750 °C [14–16]. Therefore, the hydrothermal sulfurization on the Cu-SSZ-13 samples resulted in no sulfate formation due to the high temperature. This result indicated that the high temperature SO_2 poisoning caused the catalyst to undergo permanent deactivation, different from the reversible sulfurization by sulfate-like species that takes place at low temperatures [14,17,33]. Hence, during hydrothermal aging, the main function of the added SO_2 was to increase the acidity of the gases and intensify the dealumination process, resulting in the collapse of the zeolite structure rather than forming
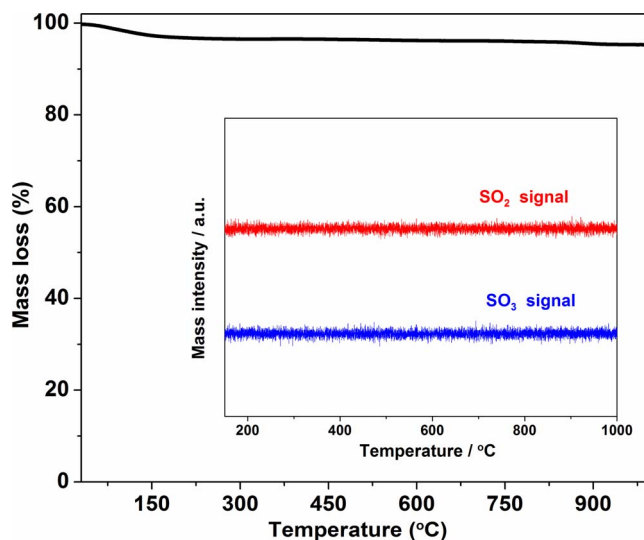

Fig. 9. TG-Mass profiles of SA-Cu-SSZ-13 catalysts. Balance of N_2 and total flow rate 50 mL/min.

sulfate species.

4. Conclusion

The deactivation mechanism of hydrothermal aging and sulfurization at high temperature has been studied for the one-pot synthesized Cu-SSZ-13 catalysts. By dislodging the extra-framework Al atoms formed during the hydrothermal aging process, the presence of SO_2 can accelerate the destruction and result in irreversible collapse of the zeolite structure for Cu-SSZ-13 catalysts at high temperatures (750 °C here). Morever, the severe deterioration of the zeolite structure caused by SO_2 promoted the loss of acid sites and accumulation of Cu^{2+} species, and these changes degraded the NH3-SCR performance of Cu-SSZ-13 catalysts.

References

[1] M. Koebel, M. Elsener, M. Kleemann, Urea-SCR: a promising techinique to reduce NOx emissions from automotive diesel engines, Catal. Today 59 (2000) 335–345.

[2] J.H. Kwak, R.G. Tonkyn, D.H. Kim, J. Szanyi, C.H.F. Peden, Excellent activity and selectivity of Cu-SSZ-13 in the selective catalytic reduction of NOx with NH3, J. Catal. 275 (2010) 187–190.

[3] J.H. Kwak, D. Tran, S.D. Burton, J. Szanyi, J.H. Lee, C.H.F. Peden, Effects of hydrothermal aging on NH3-SCR reaction over Cu/zeolites, J. Catal. 287 (2012) 203–209.

[4] Y.J. Kim, J.K. Lee, K.M. Min, S.B. Hong, I.-S. Nam, B.K. Cho, Hydrothermal stability of CuSSZ13 for reducing NOx by NH3, J. Catal. 311 (2014) 447–457.

[5] L. Xie, F. Liu, L. Ren, X. Shi, F.S. Xiao, H. He, Excellent performance of one-pot synthesized Cu-SSZ-13 catalyst for the selective catalytic reduction of NOx with NH3, Environ. Sci. Technol. 48 (2014) 566–572.

[6] D.W. Fickel, E. D'Addio, J.A. Lauterbach, R.F. Lobo, The ammonia selective catalytic reduction activity of copper-exchanged small-pore zeolites, Appl. Catal. B: Environ. 102 (2011) 441–448.

[7] J. Hun Kwak, H. Zhu, J.H. Lee, C.H. Peden, J. Szanyi, Two different cationic positions in Cu-SSZ-13? Chem. Commun. 48 (2012) 4758–4760.

[8] S.J. Schmieg, S.H. Oh, C.H. Kim, D.B. Brown, J.H. Lee, C.H.F. Peden, D.H. Kim, Thermal durability of Cu-CHA NH3-SCR catalysts for diesel NOx reduction, Catal. Today 184 (2012) 252–261.

[9] J.H. Kwak, J.H. Lee, S.D. Burton, A.S. Lipton, C.H. Peden, J. Szanyi, A common intermediate for N2 formation in enzymes and zeolites: side-on Cu-nitrosyl complexes, Angew. Chem. 125 (2013) 10169–10173.

[10] F. Gao, D. Mei, Y. Wang, J. Szanyi, C.H. Peden, Selective catalytic reduction over Cu/SSZ-13: linking homo- and heterogeneous catalysis, J. Am. Chem. Soc. 139 (2017) 4935–4942.

[11] Y. Jangjou, D. Wang, A. Kumar, J.H. Li, W.S. Epling, SO2 poisoning of the NH3-SCR reaction over Cu-SAPO-34: effect of ammonium sulfate versus other S-Containing species, ACS Catal. 6 (2016) 6612–6622.

[12] K. Wijayanti, K. Leistner, S. Chand, A. Kumar, K. Kamasamudram, N.W. Currier, A. Yezerets, L. Olsson, Deactivation of Cu-SSZ-13 by SO2exposure under SCR conditions, Catal. Sci. Technol. 6 (2016) 2565–2579.

[13] J. Luo, D. Wang, A. Kumar, J. Li, K. Kamasamudram, N. Currier, A. Yezerets, Identification of two types of Cu sites in Cu/SSZ-13 and their unique responses to hydrothermal aging and sulfur poisoning, Catal. Today 267 (2016) 3–9.

[14] A. Kumar, M.A. Smith, K. Kamasamudram, N.W. Currier, H. An, A. Yezerets, Impact of different forms of feed sulfur on small-pore Cu-zeolite SCR catalyst, Catal. Today 231 (2014) 75–82.

[15] L. Zhang, D. Wang, Y. Liu, K. Kamasamudram, J. Li, W. Epling, SO2 poisoning impact on the NH3-SCR reaction over a commercial Cu-SAPO-34 SCR catalyst, Appl. Catal. B: Environ. 156–157 (2014) 371–377.

[16] W. Su, Z. Li, Y. Zhang, C. Meng, J. Li, Identification of sulfate species and their influence on SCR performance of Cu/CHA catalyst, Catal. Sci. Technol. 7 (2017) 1523–1528.

[17] D.W. Brookshear, J.-g. Nam, K. Nguyen, T.J. Toops, A. Binder, Impact of sulfation and desulfation on NOx reduction using Cu-chabazite SCR catalysts, Catal. Today 258 (2015) 359–366.

[18] A.G. Sappok, V.W. Wong, Physical Characterization of Ash Species in Diesel Exhaust Entering Aftertreatment Systems, SAE international, 2007-01-0318, 2007.

[19] J. Park, H. Park, J. Baik, I. Nam, C. Shin, J. Lee, B. Cho, S. Oh, Hydrothermal stability of CuZSM5 catalyst in reducing NO by NH3 for the urea selective catalytic reduction process, J. Catal. 240 (2006) 47–57.

[20] M. Haouas, F. Taulelle, C. Martineau, Recent advances in application of (27)Al NMR spectroscopy to materials science, Prog. Nucl. Magn. Reson. Spectrosc. 94–95 (2016) 11–36.

[21] S. Prodinger, M.A. Derewinski, Y. Wang, N.M. Washton, E.D. Walter, J. Szanyi, F. Gao, Y. Wang, C.H.F. Peden, Sub-micron Cu/SSZ-13: Synthesis and application as selective catalytic reduction (SCR) catalysts, Appl. Catal. B: Environ. 201 (2017) 461–469.

[22] P.G. Blakeman, E.M. Burkholder, H.-Y. Chen, J.E. Collier, J.M. Fedeyko, H. Jobson, R.R. Rajaram, The role of pore size on the thermal stability of zeolite supported Cu SCR catalysts, Catal. Today 231 (2014) 56–63.

[23] D. Wang, F. Gao, C.H.F. Peden, J. Li, K. Kamasamudram, W.S. Epling, Selective catalytic reduction of NOxwith NH3over a Cu-SSZ-13 catalyst prepared by a solid-State ion-Exchange method, ChemCatChem 6 (2014) 1579–1583.

[24] F. Gao, N.M. Washton, Y. Wang, M. Kollár, J. Szanyi, C.H.F. Peden, Effects of Si/Al ratio on Cu/SSZ-13 NH3-SCR catalysts: implications for the active Cu species and the roles of Brønsted acidity, J. Catal. 331 (2015) 25–38.

[25] J. Luo, F. Gao, K. Kamasamudram, N. Currier, C.H.F. Peden, A. Yezerets, New insights into Cu/SSZ-13 SCR catalyst acidity. Part I: Nature of acidic sites probed by NH 3 titration, J. Catal. 348 (2017) 291–299.

[26] R. Zhang, J.-S. McEwen, M. Kollár, F. Gao, Y. Wang, J. Szanyi, C.H.F. Peden, NO chemisorption on Cu/SSZ-13: a comparative study from infrared spectroscopy and DFT calculations, ACS Catal. 4 (2014) 4093–4105.

[27] E.D. Gao, E.M. Walter, J. Karp, R.G. Luo, J.H. Tonkyn, J. Kwak, C.H.F. Szanyi, Structure–activity relationships in NH3-SCR over Cu-SSZ-13 as probed by reaction kinetics and EPR studies, J. Catal. 300 (2013) 20–29.

[28] F. Gao, E.D. Walter, M. Kollar, Y. Wang, J. Szanyi, C.H.F. Peden, Understanding ammonia selective catalytic reduction kinetics over Cu/SSZ-13 from motion of the Cu ions, J. Catal. 319 (2014) 1–14.

[29] I. Lezcano-Gonzalez, U. Deka, B. Arstad, A. Van Yperen-De Deyne, K. Hemelsoet, M. Waroquier, V. Van Speybroeck, B.M. Weckhuysen, A.M. Beale, Determining the storage, availability and reactivity of NH3 within Cu-Chabazite-based Ammonia Selective Catalytic Reduction systems, Phys. Chem. Chem. Phys. 16 (2014) 1639–1650.

[30] D. Wang, L. Zhang, K. Kamasamudram, W.S. Epling, In situ-DRIFTS study of selective catalytic reduction of NOxby NH3over Cu-Exchanged SAPO-34, ACS Catal. 3 (2013) 871–881.

[31] L. Xie, F. Liu, K. Liu, X. Shi, H. He, Inhibitory effect of NO2 on the selective catalytic reduction of NOx with NH3 over one-pot-synthesized Cu–SSZ-13 catalyst, Catal. Sci. Technol. 4 (2014) 1104–1110.

[32] J.H. Kwak, T. Varga, C.H.F. Peden, F. Gao, J.C. Hanson, J. Szanyi, Following the movement of Cu ions in a SSZ-13 zeolite during dehydration, reduction and adsorption: a combined in situ TP-XRD XANES/DRIFTS study, J. Catal. 314 (2014) 83–93.

[33] T. Ando, Y. Hihara, M. Banno, T. Nagata, N. Ishitsuka, T. Matsubayashi, Detailed Mechanism of S Poisoning and De-Sulfation Treatment of Cu-SCR Catalyst 1 SAE international, 2017.